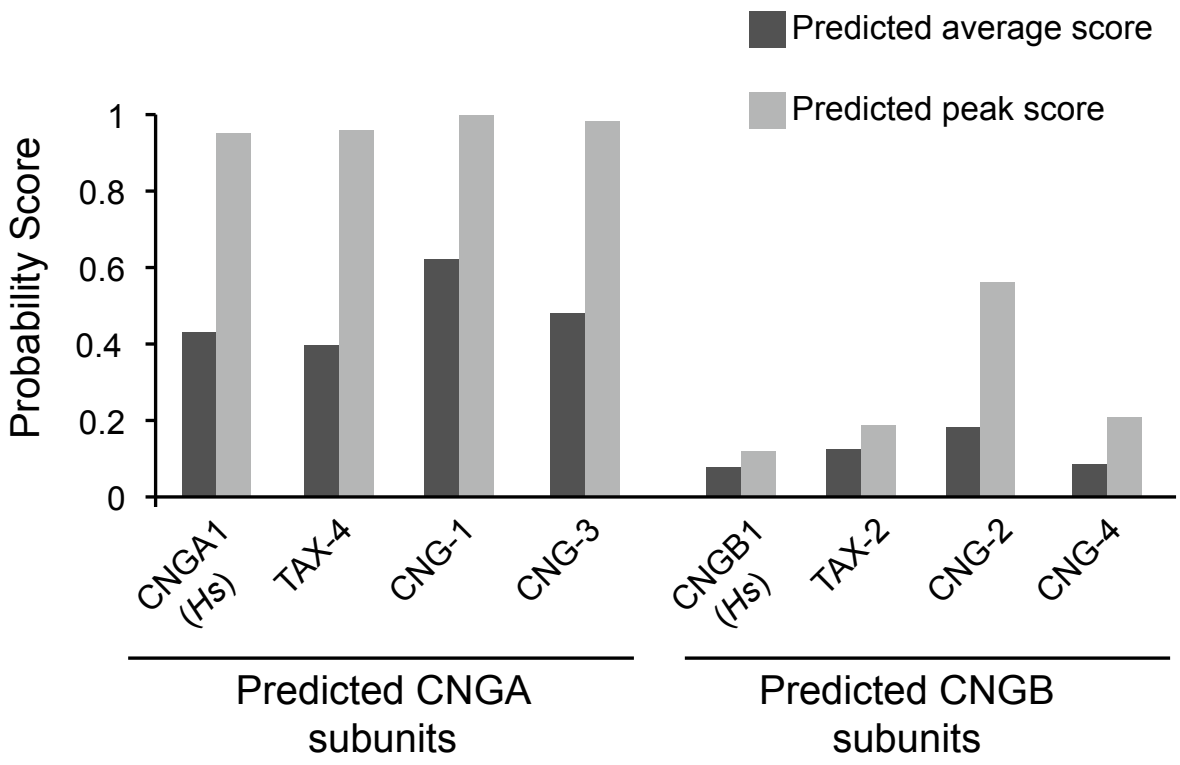

Fig. S1. Prediction of C-terminal interaction domains within CNG channel subunits. The protein sequence of each CNG channel subunit in *C. elegans* was examined for the presence of a candidate C-terminal coiled coil domain. Human (Hs) CNGA1 and CNGB1sequences were included as controls. Probability scores for predicted coiled coil motifs were obtained using COILS (http://embnet.vital-it.ch/software/coils/COILS) (Lupas et al., 1991). The average and maximum probability scores were calculated across the entire C-terminus of each CNG channel subunit. The amino acid positions for predicted coiled coil domains are: HsCNGA1 647-741; HsCNGB1 1122-1169; TAX-4 600-693; TAX-2 646-728; CNG-1 590-646; CNG-2 698-790; CNG-3 546-610; CNG-4 566-631.

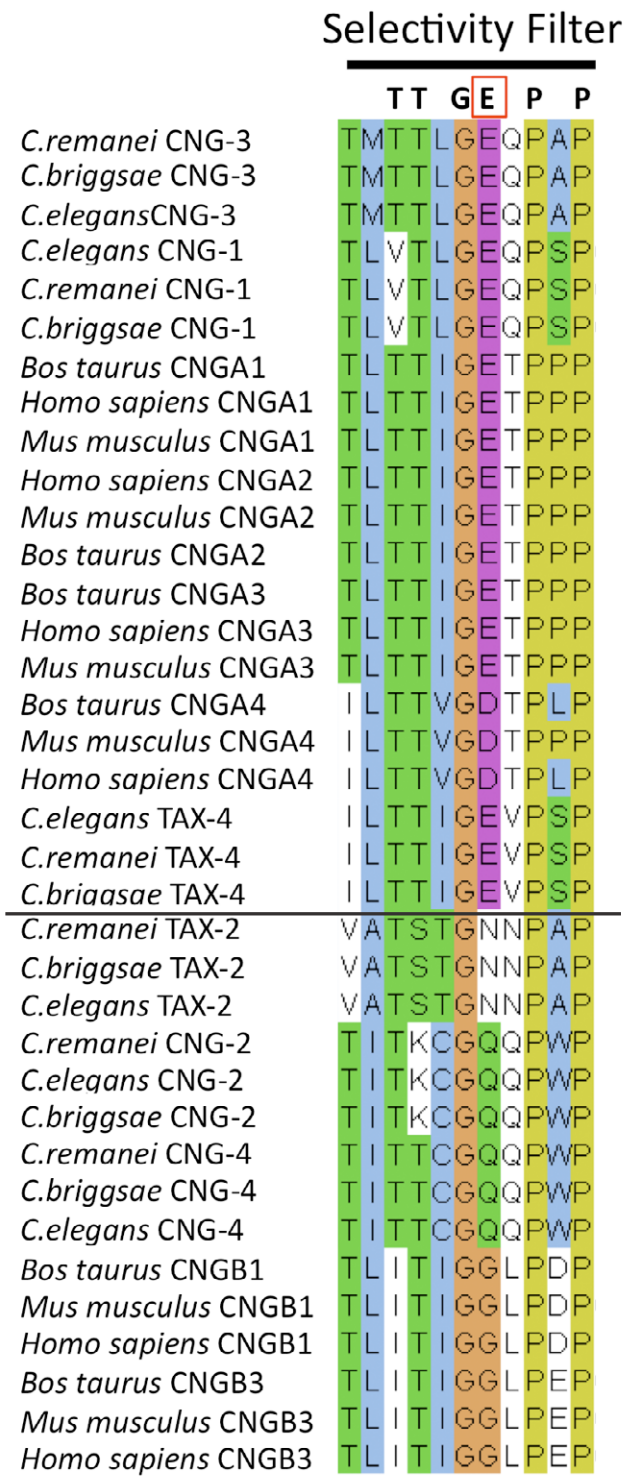

Fig. S2. Alignment of the selectivity filter region across CNG channel subunits. Alignment of selectivity filters from nematode and mammalian CNG channel subunits showing the conserved negatively charged residue (boxed E) within the domain (Contreras et al., 2008). The alignment was performed using the multiple sequence alignment software MUSCLE (Edgar, 2004).

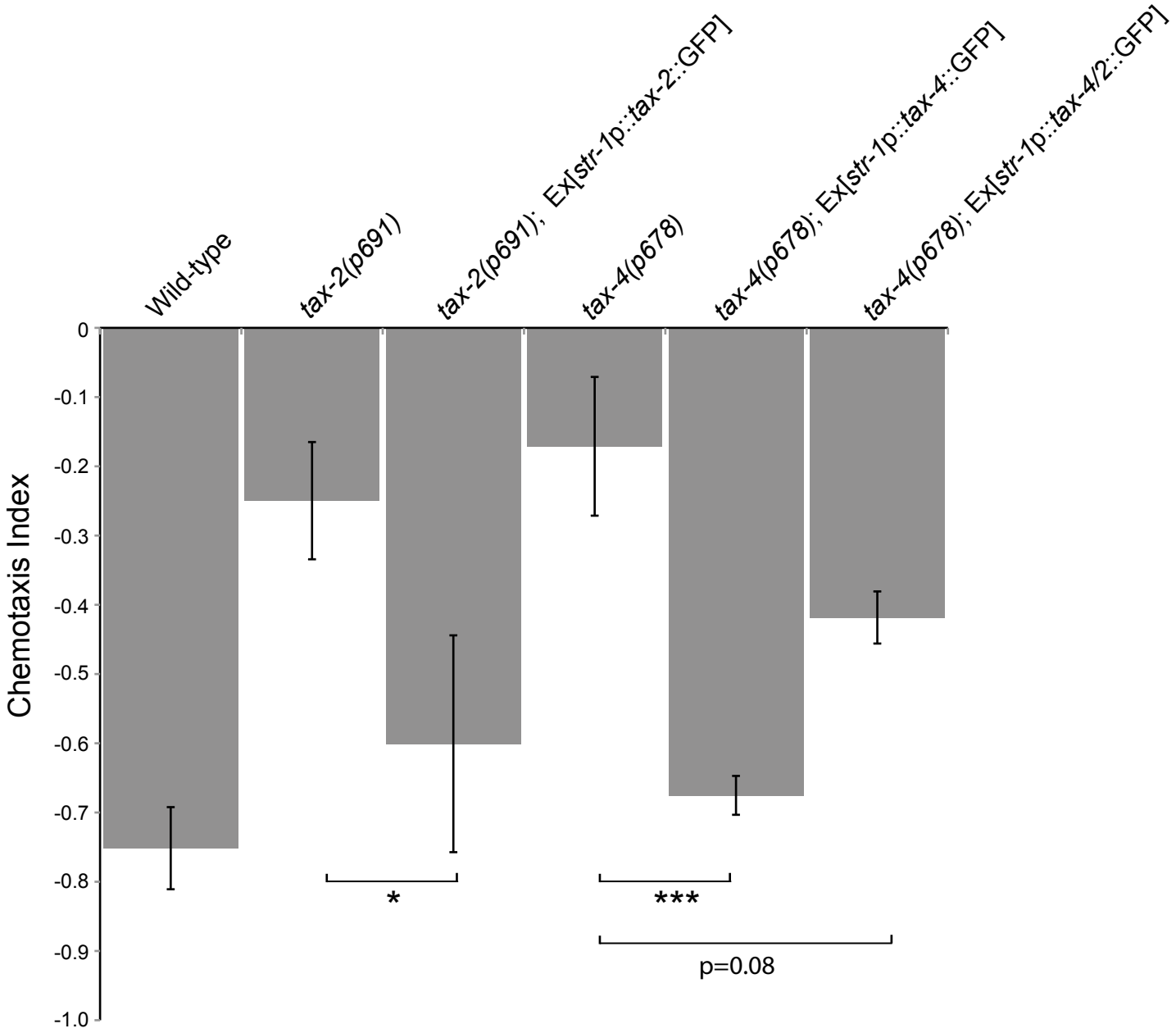

Fig. S3. TAX-2::GFP and TAX-4::GFP fusion proteins restore avoidance of 2-nonanone to *tax-2* and *tax-4* mutants, respectively. Responses of animals of the indicated genotypes to a 1:10 dilution of 2-nonanone. Fusion proteins were expressed in AWB under the *str-1* promoter. See Figure 6 for details of the TAX-4/2 chimeric protein. Chemotaxis assays were scored on three independent days. n = 3-6 assays with 50-100 animals per assay. * and *** indicate different from indicated strains at $P < 0.05$ and <0.001, respectively (ANOVA and post-hoc correction). Outliers (defined as assays with chemotaxis indices greater than two standard deviations from the mean) are not included. Error bars indicate SEM.

Table S1. Role of NPHP-2 in TAX-2 ciliary targeting in AWB.

Strain	Fusion protein examined[a]	% animals with localization to:					
		Entire cilium/ MS[b]	Cilium + distal dendrite	Distal dendrite	Cell body	No exp.	*P*-value
Wild-type	NPHP-2	0/90.5	0	0	0	9.5	
Wild-type	NPHP-2-AKR	74/0	0	0	0	26	
Wild-type[c]	TAX-2	0/98	0	0	0	2	
nphp-2(gk653)	TAX-2	13/5	0	0	7	75	<0.001[d]
nphp-2(gk653); Ex[*str-1*p::*nphp-2*-AKR]	TAX-2	10/31	4	0	0	54	<0.001[e]
daf-25(m98)	NPHP-2	0/28	0	0	0	72	<0.001[d]

[a]TAX-2 and NPHP-2 were fused to GFP or mCherry, respectively. Expression in AWB was driven under the *str-1* promoter. NPHP-2-AKR – ankyrin repeat domain of NPHP-2.
[b]MS – middle segment.
[c]Data are from Table 2.
[d]As compared to values in wild-type animals.
[e]As compared to values in *nphp-2* mutants. Note that while the differences in proportions among different categories in this strain are significantly different from those in *nphp-2* mutants, only a small subset of animals exhibit TAX-2 localization to the cilia as compared to the pattern in wild-type animals or upon rescue with full-length *nphp-2* (Table 2).
Adult animals grown at 20ºC were examined. n=12-35 animals each. Expression from the same array was examined in wild-type and mutant animals when relevant.